Uniform Self-Forming Metallic Network as a High-Performance Transparent Conductive Electrode

Bing Han, Ke Pei, Yuanlin Huang, Xiaojian Zhang, Qikun Rong, Qinggeng Lin, Yangfei Guo, Tianyi Sun, Chuanfei Guo, David Carnahan, Michael Giersig, Yang Wang, Jinwei Gao, Zhifeng Ren,* and Krzysztof Kempa**

Materials with simultaneous high electrical conductivity and optical transmittance are essential for various optoelectronic devices, such as touch-screen displays,[1–4] solar cells,[2,5–7] and organic light-emitting diodes.[2,8,9] Doped metal oxide films, such as tin-doped indium oxide (ITO) and fluorine-doped tin oxide (FTO), have dominated the field[9,10] but suffer from several critical drawbacks, including high price, scarcity of materials (e.g., indium), high processing temperatures, and brittleness.[2,11] The next generation of optoelectronic devices requires transparent conductive electrodes, which in addition to being very conductive and transparent are also mechanically flexible and compatible with large-scale manufacturing.[2,11] These problems and requirements motivate searches for new materials. Recently, development of nano-materials, such as carbon nanotubes,[1,8,12] graphene,[3,5,13] metal nanowires,[4,6,14,15] and metal grids[16,17] has opened new directions. Among these, metal nanowires combining optoelectronic advantages with low-cost manufacturing, including the roll-to-roll techniques,[2,14,15,18] lead the way for the ITO replacement.

Efforts by many groups have led to significant improvements in the performance of metal nanowire networks. In particular, the silver networks have been proposed for applications in touch-screen displays[2,4] and photovoltaic devices.[2,7,19] Silver metallic networks are normally deposited as a thin film or network from solution to form a conductive layer.[6,7,14,19] Recently, some new techniques have been developed to fabricate these structures, such as the bubble template,[20] the coffee ring effect template,[21] self assembly at a liquid interface,[22] and so on. The solution-processed methods based on random nanoparticles and nanowires offer a cheap and flexible way to fabricate the transparent conductive electrodes, but many problems still remain, such as the balance between optical and electrical conductivity, uniformity of the nanoparticles/nanowires and their distribution in a film, and the electrical contact between the nanoparticles/nanowires themselves, as well as between the metallic network and a substrate. These limits call for new, improved, and scalable approaches to fabricate metallic network films.[2,15]

In this work, we propose a new approach—based on the "cracked" gel film for making metallic networks—free of the above problems. Metallic network is evaporated/sputtered onto a template of naturally cracked gel film. The metallic network electrodes with micrometer-size pitch and silver lines, in addition to having a comparable transmittance and lower sheet resistance than ITO, are also easy to pattern and show good adhesion to flexible substrates.

Figure 1 schematically shows the processes of metallic network fabrication, which mainly includes four steps: synthesis and deposition of the TiO_2 film (as a template film), self-cracking, metallic film deposition, and template film lift-off. The resulted individual schematic images of the gel film, cracks, and the metallic network are also shown on the right side of Figure 1. An oxide gel of microcrystalline TiO_2 solution was spin-coated on a substrate of either glass or poly(ethylene terephthalate) (PET). The microcrystalline TiO_2 solution was synthesized by a normal sol-gel method.[23] In many previous applications, TiO_2 has been used as a semiconductor layer for dye-sensitized solar cells,[24,25] gas sensors,[26,27] and so on, but cracks and delamination often develop during thermal treatments,[28] and the mechanism of crack formation has been detailed elsewhere.[29,30] Here, we take advantage of this normally unwanted cracking phenomenon to form a template for the subsequent metal deposition. We optimize the microcrystalline cracking effect by low-temperature thermal processing. In addition, we have shown that similarly

B. Han,[+] K. Pei,[+] Y. Huang, X. Zhang, Q. Rong, Q. Lin, Y. Guo, Prof. Y. Wang, Prof. J. Gao
Institute for Advanced Materials (IAM)
Academy of Advanced Optoelectronics
South China Normal University
Guangzhou 510006, China
E-mail: gaojw@scnu.edu.cn

B. Han
School of Physics and Telecommunication Engineering
South China Normal University
Guangzhou 510006, China

Dr. T. Sun, Prof. K. Kempa
Department of Physics
Boston College, Chestnut Hill,
Massachusetts 02467, USA
E-mail: kempa@bc.edu

Dr. T. Sun, Dr. C. Guo, Prof. Z. Ren
Department of Physics and TcSUH
University of Houston
Houston, Texas 77204, USA
E-mail: zren@uh.edu

Dr. D. Carnahan
NanoLab, Inc., Waltham, Massachusetts 02451, USA

Prof. M. Giersig
Department of Chemistry
UAM Poznan, Poland

Prof. M. Giersig
Department of Physics
Freie Universität Berlin
Berlin 14195 , Germany Department of Physics
Freie Universität Berlin, Berlin 14195, Germany

[+]These authors contributed equally to this work

DOI: 10.1002/adma.201302950

© 2013 WILEY-VCH Verlag GmbH & Co. KGaA, Weinheim

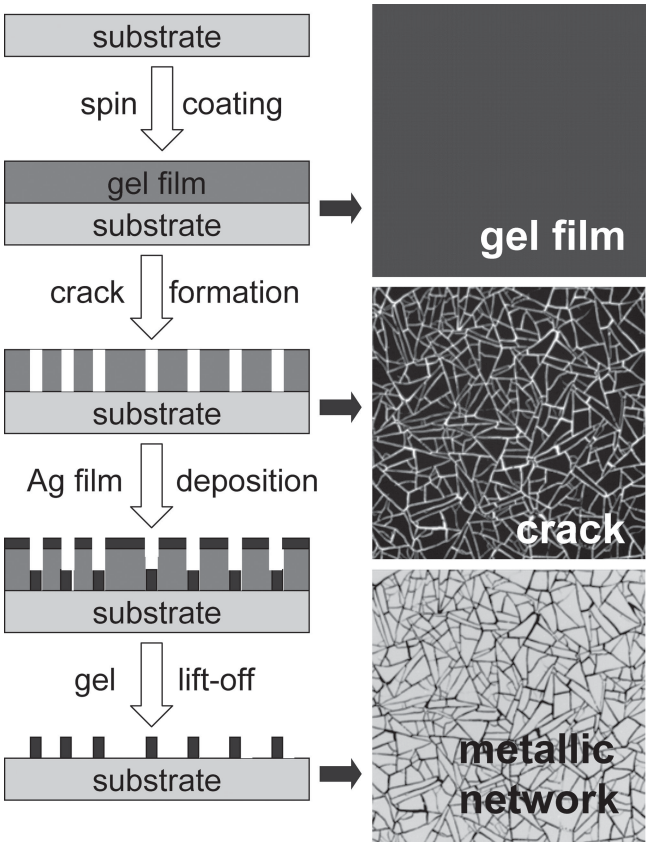

Figure 1. Schematic process of metallic network fabrication. The resulted structures of gel film, cracks and network are shown on the right column.

cracking can be achieved with other media, such as the inexpensive Lubrizol Carboset (CA 600) acrylic emulsion or even with inexpensive and environmentally friendly gelatin (**Figure 2**d shows an example of an optical image of a cracked CA 600 film). Subsequently, metal deposition was processed, followed by TiO_2 lift-off, leaving the Ag network pattern shown in Figure 1 (labeled "metallic network"). We use two different techniques for silver deposition: thermal evaporation and sputtering. Lift-off is performed by a soft mechanical wiping, followed by 1 min ultrasonication in ethanol. We have obtained different Ag network samples with different averaged pitch (varying from 4 to 100 μm) (labeled as "*w*" hereafter) and different averaged wire width (varying from 1 to 2 μm) (labeled as "*d*" hereafter). These parameters are controllable with spin coating speed, cracking temperature, and so on. A detailed correlation among the fabrication conditions, the resulting mesh morphologies, and their physical properties is listed in Table S1 of the Supporting Information.

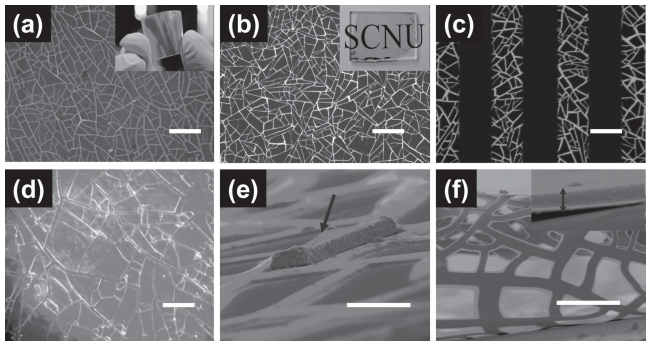

Figure 2. Optical microscope images of our Ag network on a) a flexible PET substrate and on b) a glass substrate. The inset in (a) shows a photograph of the Ag network structure on a bent PET substrate, 4 cm × 2 cm in size. The inset in (b) shows a photograph of the Ag network structure on a glass substrate, 3 cm × 2 cm in size. c) Optical microscope image of a photolithographically etched Ag networks with the width of the etched stripes of ≈50 μm. d) Optical microscope image of the "cracked" pattern in a CA 600 film. e) SEM image of Ag network at the tilt angle of ≈30°. The green arrow points to a leftover of a TiO_2 block. f) SEM image of a lifted-off Ag network on a glass substrate. The inset SEM image in (f) indicates the thickness of Ag network is about 60 nm. The scale bars in (a), (b), (c), and (d) are 50 μm, and those in (e) and (f) are 20 μm.

Figure 2a, b shows the optical microscopy images of Ag network on a flexible PET and a glass substrate, respectively. The photographs of the Ag network on the PET and glass are also shown as the insets in Figure 2a, b. Clearly, the Ag networks on both substrates are mostly transparent. The inset of Figure 2a shows a good flexibility of the Ag network that is compatible with flexible PET substrate, which is important for the flexible device applications.[1,2,4] The Ag network on PET shows an approximately smaller feature than that on glass. In this case, the Ag networks on glass and PET show different $d \approx 2$ μm and ≈1 μm, respectively, and roughly the same $w \approx 20$ μm. Such different features result in different sheet resistance and optical transmittance, as discussed in the next section. The possible reason for the different morphologies of Ag networks on PET and glass can be attributed to the different surface properties. Selective removal of a transparent conductive layer from the substrate to create circuit patterns is a necessary step for current Ag network application in the flat panel display. Figure 2c shows that patterned Ag network with its photolithographically defined pattern[17] of stripes of ≈50 μm width and spacing of ≈50 μm. Figure 2d shows an optical image of an alternative, inexpensive "cracked" template, the CA 600 film. Figure 2e shows a SEM image of the ≈30° tilted Ag network on glass, with a TiO_2 block intentionally left (green arrow). To demonstrate the nearly perfect morphology of the network, a scanning electron microscopy (SEM) image of a delaminated piece (with a blade) of the Ag network from the glass substrate is shown in Figure 2f. The inset SEM image shows that the thickness of the sputtered Ag network is ≈60 nm.

Figure 3 compares the optical transmittance (in the range of wavelength from 400 to 800 nm) of two typical Ag network electrodes (≈60 nm in thickness) with $d \approx 2$ μm and $w \approx 45$ μm for glass substrate and $d \approx 1$ μm and $w \approx 65$ μm for PET substrate, along with that of an sputtered ITO-coated film (≈150 nm in thickness) on a glass substrate. The Ag network electrodes on both glass and PET substrates exhibit good transmittance (≈88% for PET substrate, ≈82% for glass substrate, at wavelength $\lambda = 550$ nm) over 400 to 800 nm, which is comparable to commercial ITO (≈87%, at wavelength $\lambda = 550$ nm). By adjusting the *w* and *d* of the Ag network, the sheet resistance of the samples can be lowered to ≈4.2 Ω sq^{-1} with 82% transmittance, and ≈0.5 Ω sq^{-1} with ≈45% transmittance (both on glass). While an electrode with ≈45% transmittance cannot be used for solar applications, it could be an excellent choice for high sensitivity touch-screen displays, as the low transparency

© 2013 WILEY-VCH Verlag GmbH & Co. KGaA, Weinheim
Adv. Mater. **2013**,
DOI: 10.1002/adma.201302950

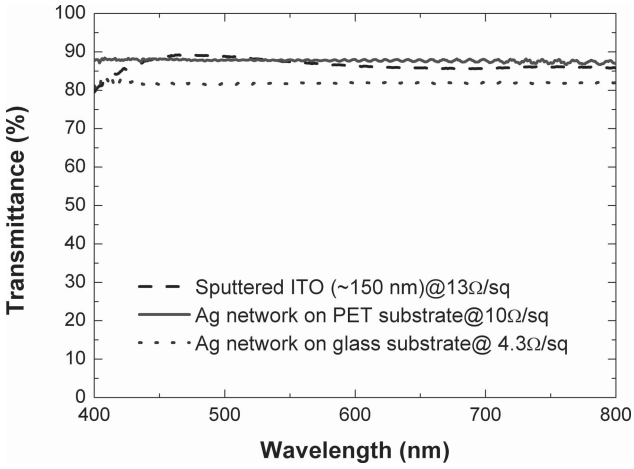

Figure 3. Optical transmittances as a function of wavelength for our Ag network on glass and PET substrate, along with that of sputtered ITO film of ≈150 nm thickness.

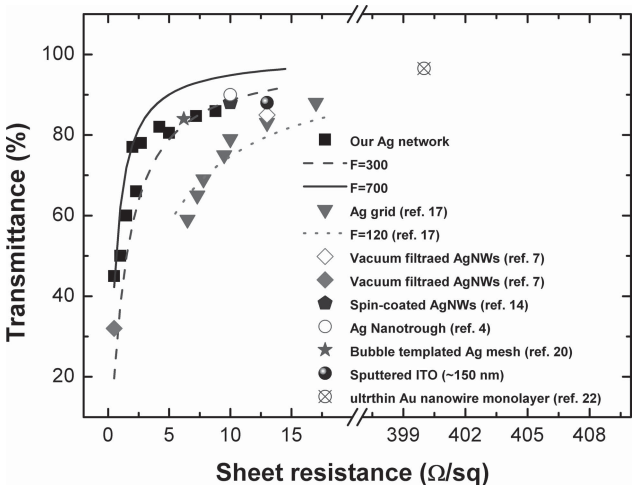

Figure 4. Optical transmittance versus the corresponding sheet resistance for our Ag network samples on glass at the wavelength $\lambda = 550$ nm, for silver nanogrid electrodes,[17] vacuum filtrated silver nanowire mesh,[7] spin-coated silver nanowire mesh,[14] Ag nanotrough,[4] and bubble templated silver mesh,[20] Au-NWs monolayer film (96.5%, 400 Ω sq^{-1}),[22] and ≈150 nm thick layer of ITO sputtered on glass. The lines represent fits of Equation (1) to the clusters of data points, which determine the corresponding fitting parameter *F*.

can be compensated by stronger back-lighting of a display. Typically a smaller line width (*d*) of Ag network assembled on PET substrates, as compared to glass (see Figures 2a,b), results in larger sheet resistance, but higher transmittance (≈10 Ω sq^{-1} at ≈88%). A detailed relationship between the structure (thickness and area coverage of metal film) and function (sheet resistance and light transmittance) is shown in the supporting information (Figures S1–S4, Supporting Information).

Typically, optical transmittance and dc conductivity change in opposite directions for transparent conductive electrode (TCE) materials.[2] The figure of merit *F*, which is defined as the ratio of the electrical to optical conductivity ($F = \sigma_{dc}/\sigma_{opt}$), where the σ_{dc} is the electrical conductance at 0 frequency, and σ_{opt} is the sheet conductance in the optical frequency range. In order to maximize the film's potential for use as a transparent conductor, it is typically desirable to have a low sheet resistance (high σ_{dc}) and a high optical transmission. The figure of merit *F* has been widely used to judge the overall performance of transparent conductive electrodes[2,17] (the larger *F* the better the performance), and is related to the transparency (*T*) and the sheet resistance (R_s) as follows[17]

$$T = \left(1 + \frac{188.5}{R_S F}\right)^{-2} \quad (1)$$

Here we use *T* at the wavelength $\lambda = 550$ nm. **Figure 4** summarizes the experimental data, by plotting the optical transmittance at 550 nm versus the sheet resistance. The *F* values were obtained by fitting Equation (1) to the experimental data (transmittance and sheet resistance). Our Ag network samples, with *d* of 1–2 μm, and *w* of 4–100 μm, have good electro-optical properties, with transmittance ranging from 82% (with ≈4.2 Ω sq^{-1} sheet resistance) to 45% (with ≈0.5 Ω sq^{-1} sheet resistance), and very high figure of merit *F* ranging from 300 to 700. Such a high figure of merit has been demonstrated before only with the bubble templated silver mesh[20] (84%, 6.2 Ω sq^{-1}), the spin-coated silver wire mesh[14] (88%, 10 Ω sq^{-1}), vacuum filtered AgNWs[7] (85%, 13 Ω sq^{-1} and 32%, 0.5 Ω sq^{-1}), Ag nanotrough[4] (90%, 10 Ω sq^{-1}), and Au-NWs monolayer film (96.5%, 400 Ω sq^{-1}).[22] Other leading published structures, such as the silver nano grid,[17] correspond to a much lower figure of merit of $F \approx 120$. Figure 4 shows that our Ag network structures achieve 76% transmittance and ≈2 Ω sq^{-1} sheet resistance, which is a very good result. Note that the Ag network on PET also has $F \approx 360$. We note that since the reflection of silver network is comparable to the absorption, as a property indicator *F* may not be as effective as it is used in the carbon nanotube cases.[2]

Figure 5a shows the sheet resistance of our Ag network structure (with $d \approx 1$ μm and $w \approx 65$ μm) on PET as a function of the bending angle. The measurement setup is shown in the inset. When the bending angle varies from –120° to 120°, constituting a slight variation in the resistance of the Ag network is observed. This variation is however reversible, even after multiple bending cycles. Also, the Ag network structure survives multiple finger-touching, simulating the potential for touch-screen use. Figure 5b, c shows a working prototype of a mechanically flexible touch screen display based on our network (letters "SCNU" were written). In addition, our network is hydrophobic, which promotes self-cleaning, which may open up a new class of potential applications.

In conclusion, we have developed an inexpensive, highly transparent, conductive, and mechanically flexible metallic network electrode via a self-formed template/mask, which contains a random but highly uniform network of line cracks for subsequent selective metal deposition. The resulting structure could be used as an excellent electrode for various flexible photonic and photovoltaic applications, exceeding the electro-optical performance of the state-of-the-art alternatives, such as ITO. We also demonstrate that our Ag network retains good conductivity under bending and shows good adhesion to various substrates.

© 2013 WILEY-VCH Verlag GmbH & Co. KGaA, Weinheim

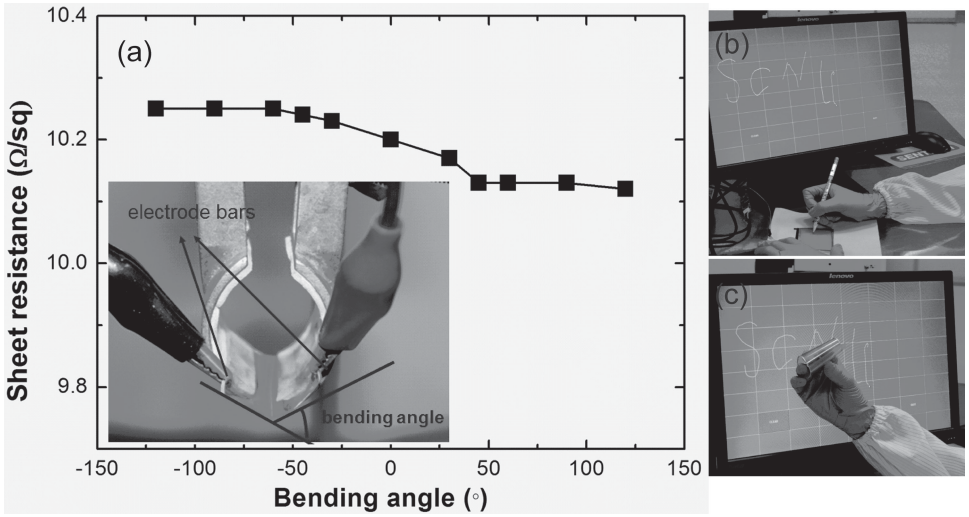

Figure 5. a) Sheet resistance of our Ag network as a function of the bending angle. Inset shows the photograph of the experimental setup of the two-probe electrical measurement. b,c) Working prototype of a mechanically flexible touch-screen display based on our metallic network, with the touch-screen writing visible on the display behind (the letters "SCNU" were written).

Experimental Section

Synthesis, Deposition, and Crack Formation—TiO_2 Films: A typical sol-gel method has been used to synthesize microcrystalline TiO_2 suspension. The general process is as follows: a solution of tetrabutyl titanate (99.9%, Kermel, China) and ethanol was prepared and added to the solution of acetic acid (99%, Kermel, China), ethanol, and diluted water under continuous stirring (1000 r min^{-1}). The solution gelled in 30 min. The stirring was stopped after the color of gel changed from light yellow to white after 1–2 h. The typical TiO_2 microcrystalline grain size is ≈100 nm. Spin coating (Spin coater, Laurell, USA) is used to deposit as-prepared TiO_2 film on substrates.

One set of samples, with the averaged wire width of 1–2 μm and pitch of 4–100 μm, were obtained by varying the concentration of precursor (0.07–0.32 g mL^{-1}), spin coating speed (1000–2000 rpm), and coating time (30–50 s). The prepared substrates with TiO_2 film were dried in air (temperature range of 25–50 °C). After several minutes, self-cracking happened.

Synthesis, Deposition, and Crack Formation—CA 600 and Gelatin Films: A chemat technology spin coater (Chemat Technology Inc. USA) was used to spin-coat a layer of Lubrizol Carboset CA 600, an acrylic, self crosslinking emulsion, onto glass slides. The slides were flooded with the emulsion and then spun at 600 rpm for 15 seconds, followed by a varied second stage. Times were varied between 15 and 50 seconds, and the speed at 1000 to 2000 rpm. The films were dried in air at 25 °C for 5 minutes. As expected, higher speeds and longer times resulted in thinner depositions, which created finer structure (i.e., more cracks) than those made at lower speed and shorter times. Additional tests made by spin-coating a gelatin resulted in similar crack networks.

Ag Film and ITO Film Deposition: Thermal evaporation (SKY Vacuum Technology Company, China), and sputtering (AJA International. ATC Orion 8, USA) were used to deposit Ag film, whereas ITO film was deposited by sputtering. The thickness of Ag film is controlled in the range of 10–120 nm (we only show samples with ≈60 nm thickness in this manuscript; the others are shown in Supporting Information), and the thickness of ITO is ≈150 nm.

Patterning of Ag Metallic Networks: A photolithograph method was used to selectively remove and pattern the as-prepared Ag networks on glass substrate, which is necessary for touch-screen display applications. A layer of negative photoresist (BN303–60) was spin-coated on the substrate with Ag networks and was subsequently followed by illuminating, developing, and baking. The silver film was etched in concentrated nitric acid (AR, Damao, China) for 1–2 min, followed by deionized water rinse three times. The as-prepared patterned fragment of the Ag networks has width and separation ≈50 μm. These dimensions (patterned fragment width and separation) can be easily varied from 1 to 100 μm with the choice of photoresist mask.

Performance Measurements: The morphologies of samples were characterized by a commercial SEM system (JEOL JCM-5700, Tokyo, Japan), a commercial optical microscope (MA 2002, Chongqing Optical & Electrical Instrument Co., Ltd). Sheet resistance of samples was measured by two methods: one is the van der Pauw method, which has four electrodes at four corners of a square (2 cm × 2 cm) of the sample and recorded with a Keithley 2400 Sourcemeter, the other is a simple setup of the two-probe electrical measurement (two fine silver paste lines (2 cm in length, 2 cm in separation) are brushed on samples), which was used to measure Ag network samples on PET substrates during bending. The sheet resistance is recorded or calculated accordingly using the above two methods. The optical transmittance was measured by integrating sphere transmittance system (Ocean Optics, USA). In this paper, all transmittance presented is the normalized value to the absolute transmittance through the substrate (glass or PET).

Touch-Screen Device Fabrication: A four-wire resistive touch-screen device was reassembled from a commercial product from TOP TOUCH Company. The 3.5-inch device consisted of a parallel ITO electrode on a PET sheet and a piece of ITO glass; in between, there is square arrays of polymer spacer dots. In this experiment, the ITO coating on PET was replaced with a high-performance silver network. The circuit was interfaced with a computer and tested the performance by a commercial controller, which was provided by the vendor.

Supporting Information

Supporting Information is available from the Wiley Online Library or from the author.

Acknowledgements

This work has been supported by Projects of "Thousands of Talents of Organization Department of the Central Committee of the CPC (2010)",

© 2013 WILEY-VCH Verlag GmbH & Co. KGaA, Weinheim

DOI: 10.1002/adma.201302950

"The Leading Talents of Guangdong Province (2011)", "China National Undergraduate Innovation Program (2012)" and NSFC under contract no. 61106061. M. G. thanks the Helmholtz Zentrum Berlin and Polish Science Foundation for the financial support.

Received: June 28, 2013
Revised: July 24, 2013
Published online:

[1] D. S. Hecht, D. Thomas, L. Hu, C. Ladous, T. Lam, Y. Park, G. Irvin, P. Drzaic, *J. Soc. Inf. Disp.* **2012**, *17*, 941.
[2] D. S. Hecht, L. Hu, G. Irvin, *Adv. Mater.* **2011**, *23*, 1482.
[3] S. Bae, H. Kim, Y. Lee, X. Xu, J. S. Park, Y. Zheng, J. Balakrishnan, T. Lei, H. R. Kim, Y. I. Song, *Nat. Nanotechnol.* **2010**, *5*, 574.
[4] H. Wu, D. Kong, Z. Ruan, P. C. Hsu, S. Wang, Z. Yu, Y. Cui, *Nat. Nanotechnol.* **2013**, *8*, 421.
[5] X. Wang, L. Zhi, K. Müllen, *Nano Lett.* **2008**, *8*, 323.
[6] J. Gao, K. Pei, T. Sun, Y. Wang, L. Zhang, W. Peng, Q. Lin, M. Giersig, K. Kempa, Z. Ren, Y. Wang, *Small* **2013**, *9*, 733.
[7] S. De, T. M. Higgins, P. E. Lyons, E. M. Doherty, P. N. Nirmalraj, W. J. Blau, J. J. Boland, J. N. Coleman, *ACS Nano* **2009**, *3*, 1767.
[8] D. Zhang, K. Ryu, X. Liu, E. Polikarpov, J. Ly, M. E. Tompson, C. Zhou, *Nano Lett.* **2006**, *6*, 1880.
[9] T. Minami, *Thin Solid Films* **2008**, *516*, 5822.
[10] K.-S. Lee, J.-W. Lim, H.-K. Kim, T. Alford, G. E. Jabbour, *Appl. Phys. Lett.* **2012**, *100*, 213302.
[11] S. Coskun, E. S. Ates, H. E. Unalan, *Nanotechnology* **2013**, *24*, 125202.
[12] S. L. Hellstrom, H. W. Lee, Z. Bao, *ACS Nano* **2009**, *3*, 1423.
[13] J. Wu, M. Agrawal, H. A. Becerril, Z. Bao, Z. Liu, Y. Chen, P. Peumans, *ACS Nano* **2009**, *4*, 43.
[14] D. S. Leem, A. Edwards, M. Faist, J. Nelson, D. D. Bradley, J. C. de Mello, *Adv. Mater.* **2011**, *23*, 4371.
[15] L. Yang, T. Zhang, H. Zhou, S. C. Price, B. J. Wiley, W. You, *ACS Appl. Mater. Interfaces* **2011**, *3*, 4075.
[16] P. B. Catrysse, S. Fan, *Nano Lett.* **2010**, *10*, 2944.
[17] J. van de Groep, P. Spinelli, A. Polman, *Nano Lett.* **2012**, *12*, 3138.
[18] A. R. Rathmell, M. Nguyen, M. Chi, B. J. Wiley, *Nano Lett.* **2012**, *12*, 3193.
[19] L. Hu, H. S. Kim, J.-Y. Lee, P. Peumans, Y. Cui, *ACS Nano* **2010**, *4*, 2955.
[20] T. Tokuno, M. Nogi, J. Jiu, T. Sugahara, K. Suganuma, *Langmuir* **2012**, *28*, 9298.
[21] M. Layani, M. Gruchko, O. Milo, I. Balberg, D. Azulay, S. Magdassi, *ACS Nano* **2009**, *3*, 3537.
[22] A. Sanchez-Iglesias, B. Rivas-Murias, M. Grzelczak, J. Perez-Juste, L. M. Liz-Marzan, F. Rivadulla, M. A. Correa-Duarte, *Nano Lett.* **2012**, *12*, 6066.
[23] H. Shin, R. Collins, M. De Guire, A. Heuer, C. Sukenik, *J. Mater. Res.* **1995**, *10*, 692.
[24] B. O'Regan, M. Grfitzeli, *Nature* **1991**, *353*, 737.
[25] K. Hara, K. Sayama, Y. Ohga, A. Shinpo, S. Suga, H. Arakawa, *Chem. Commun.* **2001**, *37*, 569.
[26] Q. Zheng, B. Zhou, J. Bai, L. Li, Z. Jin, J. Zhang, J. Li, Y. Liu, W. Cai, X. Zhu, *Adv. Mater.* **2008**, *20*, 1044.
[27] M. Li, Y. Chen, *Sens. Actuators B* **1996**, *32*, 83.
[28] N. Krins, M. Faustini, B. Louis, D. Grosso, *Chem. Mater.* **2010**, *22*, 6218.
[29] P. L. Swanson, C. J. Fairbanks, B. R. Lawn, Y. W. Mai, B. J. Hockey, *J. Am. Ceram. Soc.* **1987**, *70*, 279.
[30] Y. W. Mai, B. R. Lawn, *J. Am. Ceram. Soc.* **1987**, *70*, 289.

© 2013 WILEY-VCH Verlag GmbH & Co. KGaA, Weinheim